

# Utility & Vascular Assessment Of A Model Tissue Engineered Construct

T King, C Johnston, P Chauvin, C Tock, G Reece, C Patrick

## Citation

T King, C Johnston, P Chauvin, C Tock, G Reece, C Patrick. *Utility & Vascular Assessment Of A Model Tissue Engineered Construct*. The Internet Journal of Plastic Surgery. 2002 Volume 1 Number 2.

## Abstract

Elucidating the mechanisms of vascular assembly at the capillary level is a limiting factor in translating tissue engineering strategies to the reconstructive surgery clinic. At the 2001 NIH Bioengineering Consortium conference entitled "Reparative Medicine: Growing Tissues and Organs", the need for the development of appropriate and innovative in vivo models for studying and designing vascular networks was highlighted. We present here an initial quantitative model that proves to be sensitive to changes in vascular density, is quantitative, allows spatial and temporal measurements of the vasculature, and can be scaled from a single to a multi-component system.

## INTRODUCTION

Tissue engineering holds tremendous promise as a means for reconstructive surgery to improve patient quality of life and outcomes. A chief limiting factor in translating tissue engineering strategies to the clinic is the lack of a functional vascular network in engineered tissues. Cells and tissue assemblies greater than 150-300  $\mu\text{m}$  require a patent capillary network for the delivery of nutrients and oxygen, as well as the active transport of secreted, metabolic, and waste products.<sup>1,2,3,4,5,6,7</sup> To be sure, numerous quantitative assays have been described for measuring angiogenesis/antiangiogenesis in vivo (see review by Jain et al.<sup>8</sup>). However, current assays used to test the activation or inhibition of vascularization are not adequate for investigating tissue engineering design constraints. Quantitative, multicomponent, in vivo models are required to elucidate the fundamental mechanisms of vascular assembly. The underlying mechanisms must be understood for rational tissue engineering design.

To this end, a quantitative model tissue engineered construct (TEC) was developed. This present study reports the employment of an acellular TEC with a single component extracellular matrix (fibrin) and single component growth factor (exogenous or microsphere-delivered VEGF). TECs were implanted on two different vascular beds possessing inherently different vascular densities and capillary orientation at varied implantation times. Quantitative CD31 histometric analysis was employed to assess vascular density

( $v$ ). The model's sensitivity was assessed by determining whether differences in  $v$  could be identified upon addition of exogenous or microsphere-delivered VEGF.

## MATERIALS & METHODS

### STUDY DESIGN

Two experimental designs were utilized:

Specific procedures and details for the experimental groups listed in Tables 1 and 2 follow.

### Figure 1

Table 1: In vivo implantation sites

Implant Surface	TEC Matrix <sup>*</sup>
Muscle	VEGF(-)/Fibrin
Muscle	VEGF(+)/Fibrin
Dermis	VEGF(-)/Fibrin
Dermis	VEGF(+)/Fibrin

\* VEGF final concentration is 5 ng/mL for VEGF(+) groups

**Figure 2**

Table 2: Application of VEGF microspheres

Experimental Group	TEC Matrix
Microspheres	Fibrin + VEGF microspheres
Protein control	Fibrin + RSA microspheres
Microsphere control	Fibrin + Empty microspheres
VEGF control	Fibrin + VEGF w/out microspheres

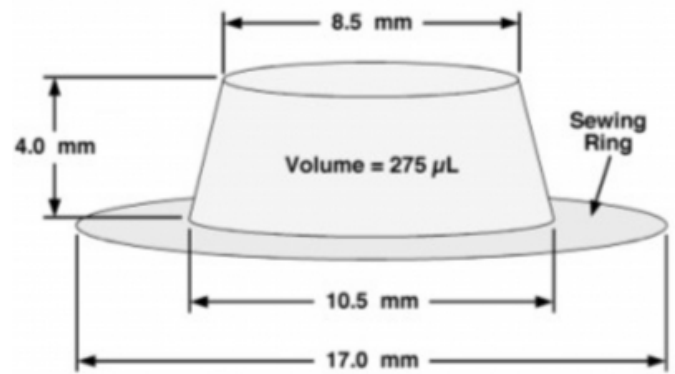
VEGF = Vascular Endothelial Growth Factor, RSA = rat serum albumin

**TEC FABRICATION**

The model TEC's design was based, in part, on an initial concept of Dvorak et al., The TEC shell was constructed from polypropylene film using a matched die mold in a heated horizontal press. The TEC is designed to be radially symmetric to enable future mathematical modeling. The utilization of polypropylene as the shell limits the invasion of tissue into a single surface of the TEC. The internal TEC diameter measures 10.5 mm, tapering to 8.5 mm over a height of 4 mm (Fig. 1). The integral sewing ring extends off of the 10.5 mm diameter end for an additional 3.5 mm, making the total diameter 17 mm. The TECs were sterilized with 100% ethanol and allowed to air dry prior to applying fibrin gels. Fibrin was selected as an initial single component ECM for this study. On the day of implantation, each TEC was filled with Tisseel® Fibrin Sealant (Baxter-Hyland, Glendale, CA) using sterile technique under a tissue culture hood. The Tisseel® system employs a duplo-syringe, one side containing standardized fibrinogen and the other containing standardized thrombin and CaCl<sub>2</sub>. For TECs containing endogenous VEGF (rhVEGF165, R&D Systems, Minneapolis, MN), the growth factor was added as an aqueous solution to the fibrinogen syringe of the Tisseel® system prior to injecting the fibrin into the TEC. The final VEGF concentration was 5 ng/mL.

**Figure 3**

Fig. 1: Schematic diagram of the model TEC.



**MICROSPHERE FABRICATION**

Microsphere manufacture using the solid encapsulation/single emulsion/solvent extraction technique and VEGF loading was performed as previously described in detail.<sup>10,11</sup> The fabrication protocol results in biodegradable polymer microspheres that contain numerous microdomains of encapsulated VEGF (see Movie).

Microspheres containing rhVEGF165 (R&D Systems, Minneapolis, MN) were manufactured by co-encapsulating the VEGF with rat serum albumin (RSA) as a carrier protein. The ratio of VEGF:RSA (w/w) was 1:2,000. The VEGF-loaded microspheres release 70 ng/mL of VEGF at 4 days, followed by a steady state VEGF concentration =5 ng/mL for at least 28 days.<sup>10</sup> For the VEGF-loaded microsphere study, all TECs were implanted on skeletal muscle.

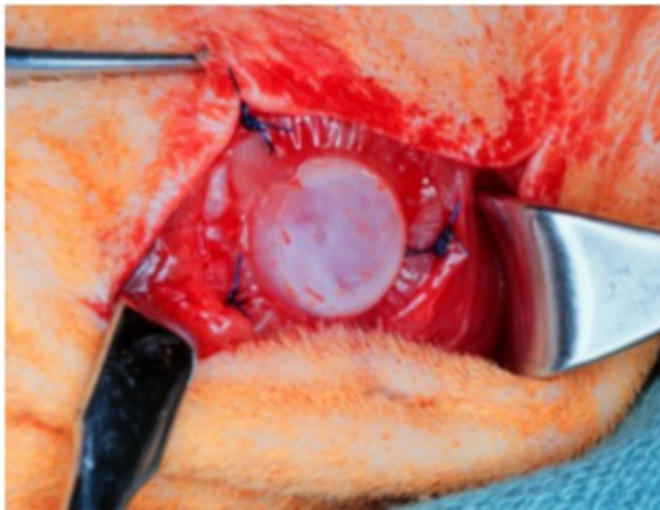
**IN VIVO IMPLANTATION**

TEC implantation was conducted as previously described.<sup>12</sup> To determine the model's sensitivity in assessing vascular density (  $\nu$  ), TEC implants were placed in two different anatomical sites (dermis and skeletal muscle) that possess different  $\nu$  and global capillary direction. Skeletal muscle possesses a higher  $\nu$  than dermis in the rat. Moreover, capillaries in the skeletal muscle are largely in the direction of muscle fibers, that being tangent to, rather than perpendicular to, the TEC's open surface. A longitudinal skin incision was made along the spine and using blunt dissection, the skin was separated from the underlying tissue. For implants on the dermis, the panniculus carnosus (cutaneous trunci) muscle was removed and, if necessary, pressure was used to achieve hemostasis. For TEC implantation on skeletal muscle, a uniform muscle surface on the back was exposed and the thin fascia covering the muscle body was removed. The TEC was sutured directly

onto the exposed uniform muscle body (rather than multiple muscle bellies) as described above (Fig. 2). Each rat received four TECs, one from each experimental group shown above in Table 1. Four animals per time point were selected based upon preliminary experimental evaluation and power-law analysis (data not shown).

**Figure 4**

Fig. 2: Perioperative view of fibrin-filled TEC sutured to skeletal muscle.



**SAMPLE EXPLANTATION**

Animal euthanasia and harvest were conducted as previously described. Post-implantation days ranging from 5 to 14 days were selected as timepoints for TEC explantation. The selection of time points for explantation was based on previous wound healing investigations demonstrating capillary extension in 3-4 days and quiescence by 21 days.<sup>9,13</sup> Thus, explantation timepoints of 5-14 days were selected based on expected rates of neovascularization and the degradation rates of the fibrin.<sup>14,15</sup>

**QUANTITATIVE IMMUNOHISTOCHEMICAL EVALUATION**

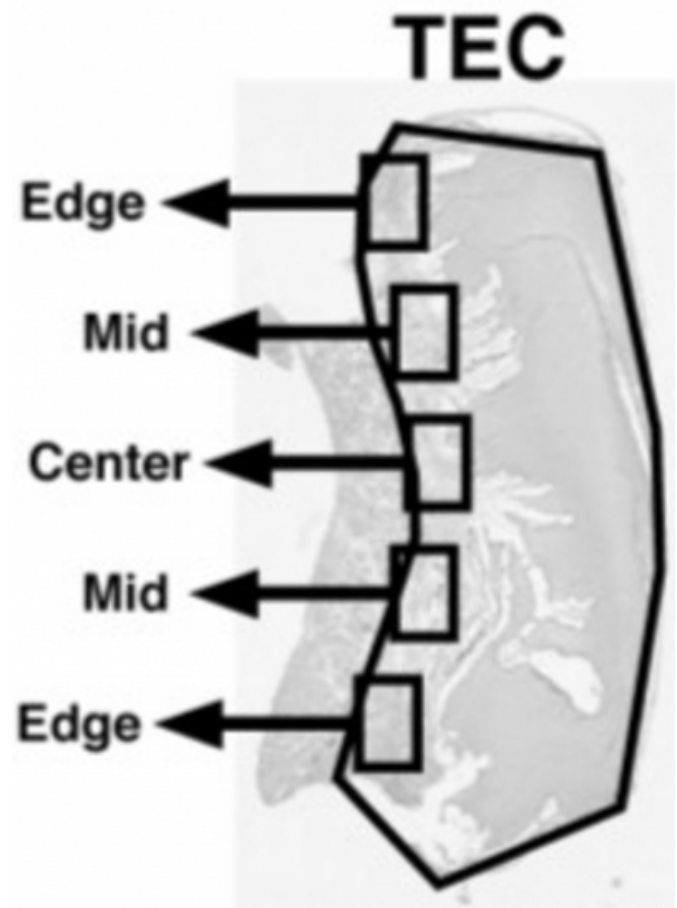
The CD31 staining protocol, digital imaging and microscopy, and quantitative assessment of vascular density were conducted as previously described in detail.<sup>12,16</sup> For each tissue section, five equally-spaced images were obtained along the interface of the implanted TEC and adjacent tissue surface (either dermis or muscle, Fig. 3). The underlying native tissue was not included in the image. The two lateral images of the TEC were labeled “edge”, the central image was labeled “center”, and the remaining two internal images were labeled “mid”. The total area of CD31 positive vasculature was calculated for each TEC image

(total of 5 TEC) using image analysis software and a previously reported semi-automated thresholding technique.<sup>12,16</sup> The  $v$  is defined as the ratio of the mean of the CD31 positive area to the total TEC area.

Data are presented in two formats: (1) the pooled  $v$  for each TEC (i.e. the mean of all analyses for each TEC regardless of geometric location within the TEC) and, (2) the  $v$  stratified to the geometric location within the TEC. Results are expressed as the mean  $\pm$  SEM for four experiments. Statistical analysis was performed by the student t-test and one-way ANOVA with Newman-Keuls multiple comparison post hoc test. Statistical significance was defined as  $p = 0.05$ .

**Figure 5**

Fig. 3: Cross-section of explanted fibrin-filled TEC (outlined) on muscle (tissue left of outline) depicting the areas of histometric analysis.



**RESULTS**

**GROSS OBSERVATIONS**

The TECs were intact and none of the implantation sites demonstrated hematoma or seroma at the time of explantation. Furthermore, all of the TECs were adherent to

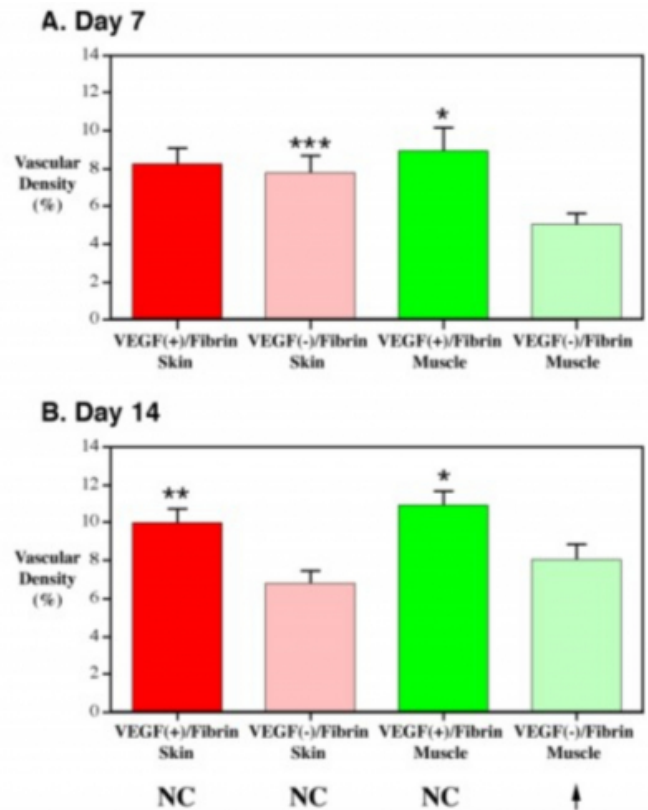
their respective implantation site at the time of explant. That is, there was no observed void space between the TEC and site of implantation. In addition, the surrounding tissues showed no signs of inflammation, infection, or gross atypia. The fibrin matrix within the TECs was present at all experimental timepoints. However, the volume of matrix present diminished with respect to time.

**DERMIS VS MUSCLE AS TEC RECIPIENT SITE ± VEGF**

Two implantation sites were compared in this investigation. It was hypothesized that there would be a difference in the TEC v as a function of the implantation site. The skin implantation site refers to the inferior dermal surface of skin overlying the medial back of the animal model. This was compared to implantation on skeletal muscle adjacent to the dermal implantation on the back. After 7 days of implantation there was a significantly greater total v in the VEGF(-)/Fibrin TECs implanted on the skin when compared to VEGF(-)/Fibrin TECs implanted on the muscle. However, after 14 days of implantation, no significant difference in total v was observed when comparing experimental groups based on implantation site (i.e. VEGF(+)/Fibrin-skin vs. VEGF(+)/Fibrin-muscle and VEGF(-)/Fibrin-skin vs. VEGF(-)/Fibrin-muscle; Fig. 4). Comparison of total v between VEGF(+)/Fibrin TECs and VEGF(-)/Fibrin TECs demonstrated increases in v (Fig. 4). The skeletal muscle implants demonstrated significantly increased v at 7 and 14 days, and the skin implants demonstrated significantly increased v by day 14. Temporally (i.e. comparing day 7 to day 14) there was a significant increase in the total v of the VEGF(-)/Fibrin TECs implanted on muscle (Fig. 4, bottom).

**Figure 6**

Fig. 4: Angiogenesis expressed by v within the TEC. (A) Day 7, (B) Day 14. The data are represented as mean  $\bar{x} \pm$  SEM. \* and \*\* denote a  $p < 0.05$  and a  $p < 0.01$ , respectively, for VEGF(+)/Fibrin vs. VEGF(-)/Fibrin groups of the same anatomical location. \*\*\* denotes a  $p < 0.05$  for VEGF(-)/Fibrin-skin vs. VEGF(-)/Fibrin-muscle. NC denotes no change in the v comparing day 7 to day 14. The vertical arrow denotes a significant increase in v comparing day 7 to day 14.

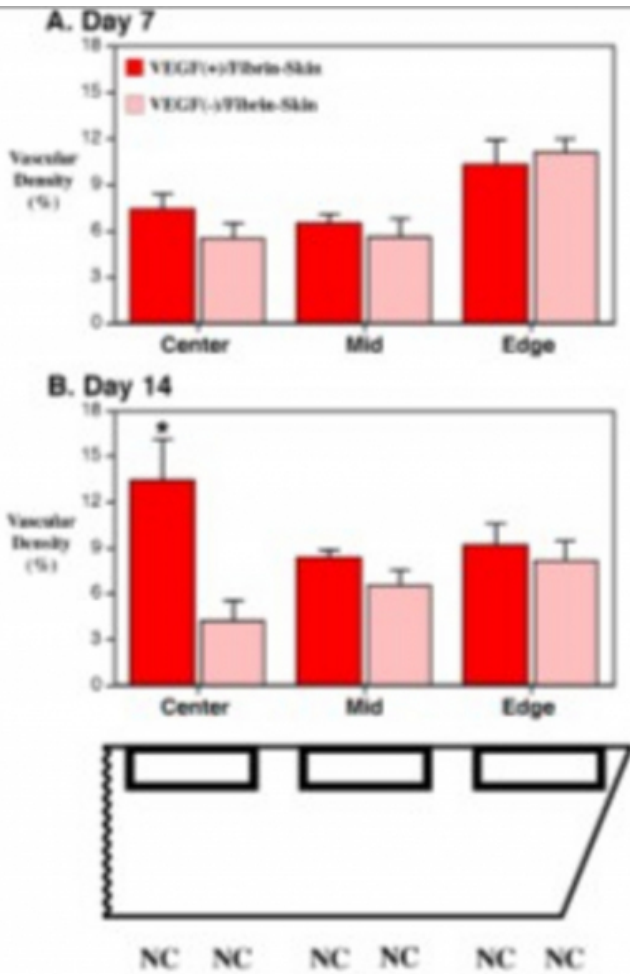


During the course of image analysis, trends in location of vascularization were noted. In Figs. 5 and 6, the total v have been stratified to location within the TEC. Figs. 5A and 5B represent the relative v of TECs implanted on skin at 7 and 14 days, respectively. Initially, at 7 days of implantation, the v at the edge of the TEC was significantly increased in the VEGF(+)/Fibrin TECs when compared to VEGF(-)/Fibrin TECs. However, by 14 days of implantation, the central region of the VEGF(+)/Fibrin TECs had developed a significantly greater v when compared to VEGF(-)/Fibrin TECs. Figs. 6A and 6B demonstrates similar trends at the skeletal muscle implantation site. In this case, VEGF(+)/Fibrin TECs demonstrated a significant increase in v at the edge of the TEC at day 7 and a significant increase in v in the central region at day 14 when compared to VEGF(-)/Fibrin TECs. Temporally, there was a significant increase in v at the edge of the TEC for fibrin implants on

muscle when comparing day 7 to day 14.

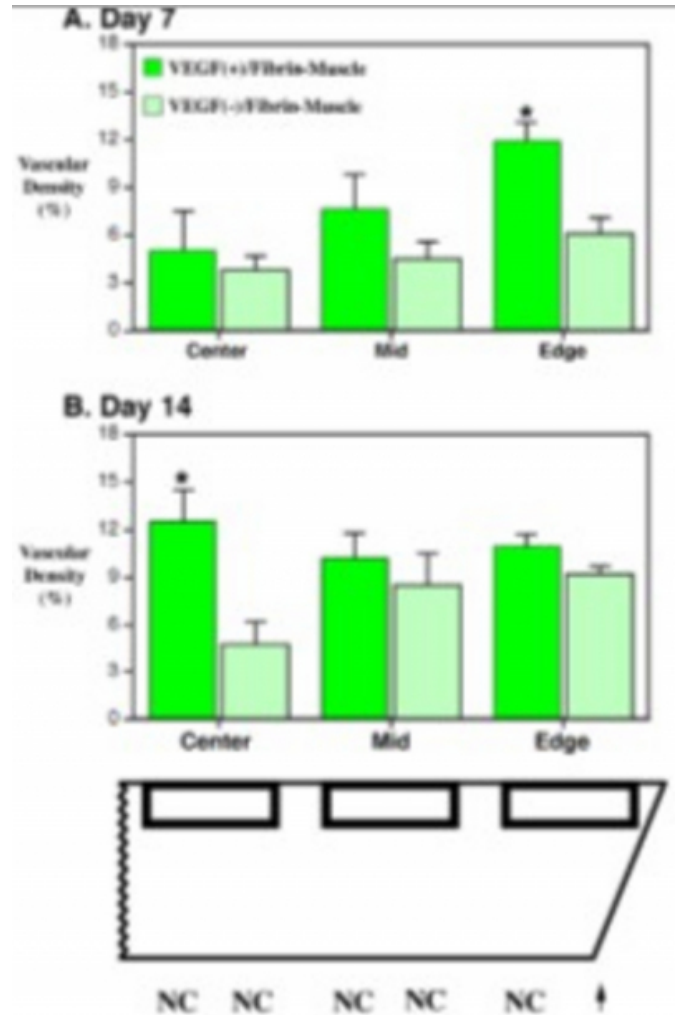
**Figure 7**

Fig. 5: Angiogenesis expressed by v with respect to position within the TEC for skin implants at (A) day 7 and (B) day 14. The data are represented as mean  $\hat{A} \pm$  SEM. \* denotes a  $p < 0.05$  for VEGF(+)/Fibrin vs. VEGF(-)/Fibrin groups of the same TEC location. The cartoon represents the location of the data within the TEC. NC denotes no change in the v comparing day 7 to day 14.



**Figure 8**

Fig. 6: Angiogenesis expressed by v with respect to position within the TEC for muscle implants at (A) day 7 and (B) day 14. The data are represented as mean  $\hat{A} \pm$  SEM. \* denotes a  $p < 0.05$  for VEGF(+)/Fibrin vs. VEGF(-)/Fibrin groups of the same TEC location. The cartoon represents the location of the data within the TEC. NC denotes no change in the v comparing day 7 to day 14. The vertical arrow denotes a significant increase in v comparing day 7 to day 14.



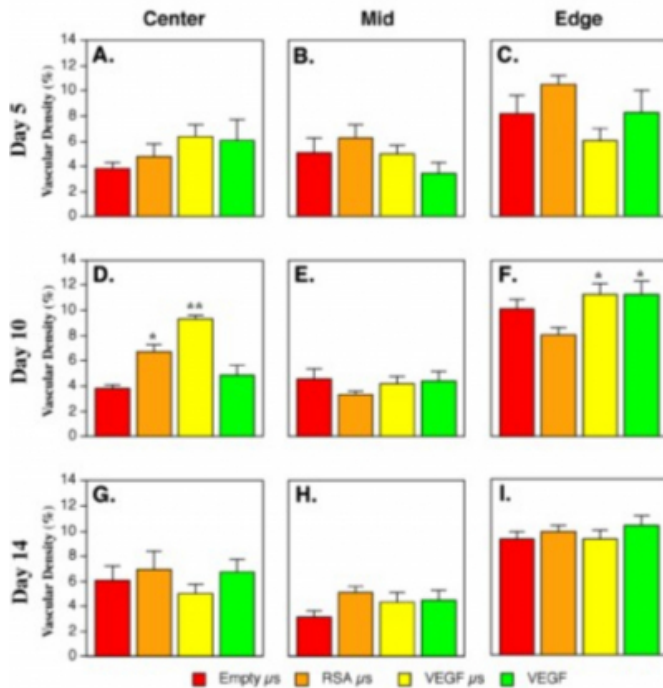
**MODULATION OF VASCULAR DENSITY VIA VEGF-LOADED MICROSPHERES**

Overall, total vascular density within all experimental groups was greater than 5% for all timepoints (data not shown). Comparatively, vascular density of rat skeletal muscle averaged 2-3% (data not shown). Stratifying the data to physical location within the TEC reveals no statistical difference in vascular density with respect to physical location within the TEC at Day 5 (see Fig. 7A-C). By day 10, the VEGF microspheres had a significantly greater vascular density at both the center and edge of the TEC (see Fig. 7D-F). At the center of the TEC, the VEGF

microspheres had significantly greater vascular density as compared to all other groups. The RSA microspheres had a significantly greater vascular density at the center when compared to empty microspheres and VEGF protein. In addition, both the VEGF microspheres and VEGF protein had a significantly greater vascular density at the edge when compared to RSA microspheres. However, by day 14 there is no statistical difference in vascular density with respect to physical location within the TEC (see Fig. 7G-I).

**Figure 9**

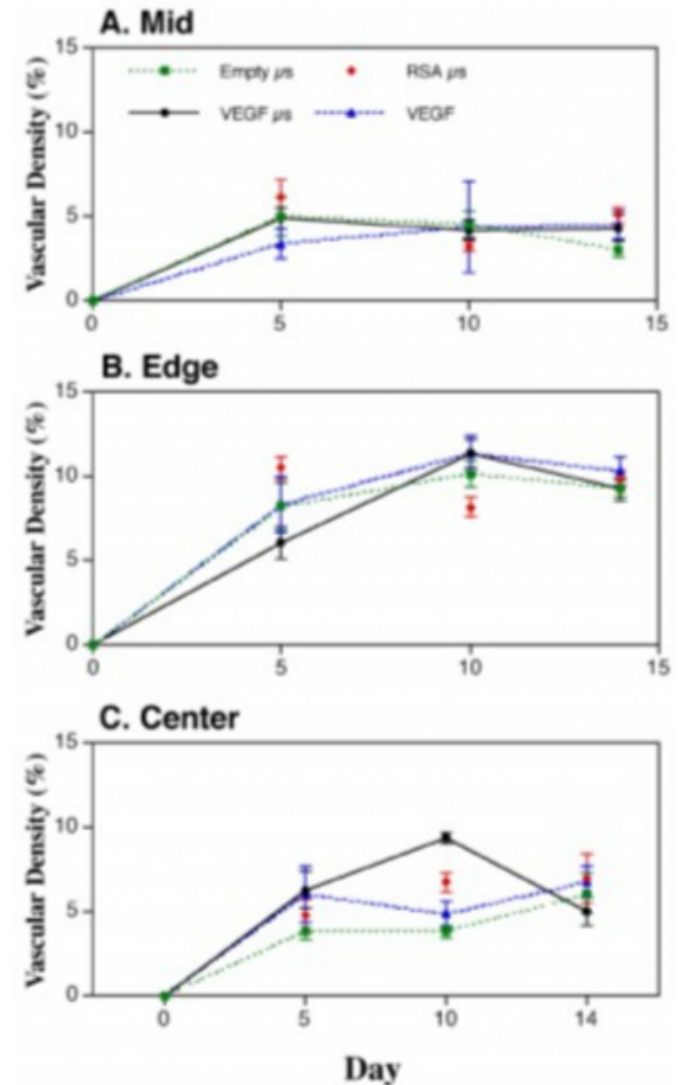
Fig. 7: Vascular Density of TECs With Respect to TEC Geometry and Time. The legend refers to the type of TEC implanted. That is, Empty  $\hat{A}\mu s$  = TECs containing empty microspheres; RSA  $\hat{A}\mu s$  = TECs containing RSA microspheres; VEGF  $\hat{A}\mu s$  = TECs containing VEGF microspheres; VEGF = TECs containing VEGF protein. Data are mean  $\hat{A}\pm$  SEM. \*\* represents a  $p < 0.01$  and \* represents a  $p < 0.05$  as derived from ANOVA analysis.



Comparisons of vascular density changes within each experimental group with respect to time of implantation are presented in Fig. 8. A significant increase in vascular density was observed in the center of VEGF-encapsulated microsphere TECs between the 5 day and 10 day timepoints. There was no statistical difference between TECs filled with fibrin alone and TECs filled with fibrin + empty microspheres.

**Figure 10**

Fig. 8: Vascular Density Within TECs Over Time. For TEC location (A) Mid, (B) Edge, (C) and Center. Note the increased relative rate of angiogenesis at the center of the TEC for the VEGF microspheres between day 5 and 10. \* represents a  $p < 0.05$  as described by ANOVA analysis.



**DISCUSSION**

All model TECs displayed angiogenesis during the observed time period as expected. A goal of this study was to determine whether differences in v could be identified in the in vivo model upon addition of exogenous growth factors. In the first configuration, exogenous VEGF was mixed with fibrin. Overall, a significant increase in v was apparent when comparing pooled data from VEGF(+)/Fibrin TECs and VEGF(-)/Fibrin TECs. Specifically, the VEGF(+)/Fibrin TECs implanted on muscle demonstrated significantly more angiogenesis at both day 7 and 14. The significant growth shifted from the edge of the TEC at day 7 to the center of the TEC by day 14. VEGF(+)/Fibrin TECs implanted on the

dermis also demonstrated a significant increase in  $v$  at day 14. This increase was most significant at the center of the TEC.

These results demonstrate that fibrin containing VEGF protein can increase the  $v$  within TECs. The release of VEGF protein directly from the fibrin gel was initially assumed to occur rapidly after implantation. However, VEGF165 binds to ECM components and may bind to fibrin. Specifically, VEGF165 contains several basic domains as well as heparin binding domains.<sup>17</sup> A significant fraction of secreted VEGF165 is either bound to the cell membrane or sequestered in the ECM.<sup>18</sup> Sakiyama-Elbert and Hubbell have demonstrated the controlled release of bFGF (another heparin-binding growth factor) from fibrin gels by covalently binding a C-terminal heparin-binding domain to the fibrin matrix.<sup>19,20</sup> The results presented here suggest that fibrin itself may act as a biodegradable, sustained release material for VEGF.

In the second configuration, the kinetics of neovascularization was affected by the presence of VEGF microspheres within a model TEC. The TECs containing VEGF microspheres demonstrated a significant increase in vascular density at day 10 at both the edge and center of the TEC when compared to all other groups. In addition, TECs containing the RSA microspheres had a significantly higher vascular density in the center of the TEC at day 10 when compared to TECs containing VEGF protein (not microsphere released) or empty microspheres. Furthermore, TECs containing VEGF protein and VEGF microspheres had a significantly higher vascular density when compared to RSA microspheres at the edge of the TEC on day 10. These results demonstrate that the VEGF microspheres stimulate vascular ingrowth within the center of the TEC. Comparing each experimental subgroup over the duration of this investigation shows the VEGF microspheres had a significant increase in vascular density between days 5 and 10, and a significant decrease in vascular density between days 10 and 14, both at the center and edge of the TEC. Thus, VEGF microspheres increase both the vascular density and the relative rate of angiogenesis in the center of the TECs by day 10 of *in vivo* implantation. However, this increase in vascular density is unsustainable. By day 14, the TECs containing VEGF microspheres have the same vascular density as the controls at all three sites.

The TEC  $v$  observed in this investigation were greater than those observed in native tissue. Using the same

immunohistochemical and imaging techniques described in the methods, the native tissues (i.e. dermis and skeletal muscle) were found to have  $v$  of 2-3% (data not shown) while TEC  $v$  ranged from 4-13%. Concerning the temporal sustainability of the vascular networks within the TECs, in all cases the  $v$  at day 7 was sustained at day 14. That is, there was no significant decrease in  $v$  (i.e. there was no significant vascular pruning) within the TECs between days 7 and 14. This result is important as it demonstrates that the angiogenesis occurring in the first seven days is sustained and might be able to support parenchymal cell incorporation into the TEC. Further investigations need to be conducted to determine if the  $v$  would be maintained beyond 14 days of implantation.

The results of these investigations can be applied to the further development of clinically relevant tissue engineered constructs for use in humans. Many issues need to be addressed in order to successfully develop engineered tissues for human use. Other geometric designs of the model TEC might yield a more ideal conformation for the development of engineered tissues. An example of this variation in geometry is the TEC design of Miller in which a matrix of needles are used to create a series of channels that can be used to inject parenchymal cells at the appropriate timepoint.<sup>21</sup> Moreover, the model TEC can be employed to elucidate the unknown cellular and molecular mechanisms of vascular assembly at the capillary level.

## CONCLUSIONS

This initial study focused on characterizing a single component extracellular matrix (fibrin), single component growth factor (VEGF), and acellular TEC. VEGF was delivered via two vehicles, namely exogenous distribution in fibrin and VEGF-loaded microspheres. Two different implantation sites were employed. Vascular density was quantitatively determined to elucidate whether the model was sensitive enough to reflect modification to angiogenesis. Specifically,

In conclusion, this project resulted in the development of an *in vivo* model TEC for elucidating mechanisms of vascular assembly. Further studies will expand the level of complexity of the model to a multicomponent system by incorporating multiple extracellular matrices, cell types (parenchymal and/or microvascular endothelial cells), and appropriate growth factor cocktails.

## ACKNOWLEDGEMENTS

This work was supported, in part, by a Whitaker Foundation Grant (CWP), National Institutes of Health grant, HL62341 (CWP), Army DOD grant, DAMD17-99-1-9268 (CWP), and The University of Texas M.D. Anderson Cancer Center core grant from the National Cancer Institute, CA-16672.

### References

1. Folkman, J., Hochberg, M. Self regulation of growth in three dimensions. *J Exp Med* 138, 745-753, 1973.
2. Vacanti, J.P., Morse, M.A., Saltzman, W.M., Domb, A.J., Perez-Atayde, A., Langer, R. Selective cell transplantation using bioabsorbable artificial polymers as matrices. *J Pediatric Surg* 23, 2-9, 1988.
3. Dempster, W.J., Doniach, I. The survival of thyroid implants in relation to thyroid deficiency. *Arch Int Pharmacodyn* 101, 398-414, 1955.
4. Heslop, B.F., Zeiss, I.M., Nesbit, N.W. Studies on transference of bone. I. A comparison of autologous and homologous bone implants to osteocyte survival, osteogenesis, and host reaction. *Br J Exp Pathol* 41, 269-287, 1960.
5. Campbell, A.K., Hales, C.N. Maintenance of viable cells in an organ culture of mature rat liver. *Exp Cell Res* 68, 33-42, 1971.
6. Smith, P.F., Krack, G., McKee, R.L., Johnson, D.G., Gandolfi, A., Hruby, V.J., Krumdeik, C.L., Brendl, K. Maintenance of adult rat liver slices in dynamic organ culture. *In Vitro Cell Dev Biol* 22, 706-712, 1986.
7. Berthiaume, F. Tissue engineering. In: Bronzino, J.D., ed. *The Biomedical Engineering Handbook*. Boca Raton: CRC Press, 1995, pp. 1556.
8. Jain, R.K., Schlenger, K., Hockel, M., Yuan, F. Quantitative angiogenesis assays: Progress and problems. *Nature Medicine* 3, 1203-1208, 1997.
9. Dvorak, H.F., Harvey, V.S., Estrella, P., Brown, L.F., McDonagh, J., Dvorak, A.M. Fibrin containing gels induce angiogenesis: Implications for tumor stroma generation and wound healing. *Lab Invest* 57, 673-686, 1987.
10. King, T.W., Patrick Jr., C.W. Development and in vitro characterization of vascular endothelial growth factor (VEGF)-loaded poly(DL-lactic-co-glycolic acid)/poly(ethylene glycol) microspheres using a solid encapsulation/single emulsion/solvent extraction technique. *J Biomed Mater Res* 51, 383-390, 2000.
11. King, T.W., Patrick Jr., C.W. Development of growth factor-loaded poly(DL-lactic-co-glycolic acid)/poly(ethylene glycol) microspheres using a solid encapsulation/single emulsion/solvent extraction technique (patent pending, SN 09/671,540, filed 9/27/00).
12. Brey, E.M., King, T.W., Johnston, C., McIntire, L.V., Reece, G.P., Patrick Jr., C.W. A technique for quantitative 3D analysis of microvascular networks. *Microvasc Res*, in press.
13. Padera, R., Colton, CK. Time course of membrane microarchitecture-driven neovascularization. *Biomaterials* 17, 277-284, 1996.
14. Yamada, K., Clark, RAF. Provisional matrix. In: Clark, R.A.F., ed. *The Molecular and Cellular Biology of Wound Repair* (ed 2nd). New York: Plenum Press, 1996, pp. 51-93.
15. Baxter Healthcare Corporation. Tisseel VH Kit. Glendale, CA: 1998.
16. King, T.W., Brey, E.B., Youssef, A.A., Johnston, C., Patrick Jr., C.W. Quantification of vascular density using a semi-automated technique for immuno-stained specimens. *Analyt Quant Cytol Histol* 24, 39-48, 2002.
17. Veikkola, T., Alitalo, K. VEGF's receptors and angiogenesis. *Sem Cancer Biol* 9, 211-220, 1999.
18. Park, J., Keller, GA, Ferrara, N. The vascular endothelial growth factor (VEGF) isoforms: differential deposition into the subepithelial extracellular matrix and bioactivity of extracellular matrix-bound VEGF. *Molec Biol Cell* 4, 1317-1326, 1993.
19. Sakiyama, S., Schense, JC, Hubbell, JA. Incorporation of heparin-binding peptides into fibrin gels enhances neurite extension: an example of designer matrices in tissue engineering. *FASEB J* 13, 2214-2224, 1999.
20. Sakiyama, S., Hubbell, JA. Development of fibrin derivatives for controlled release of heparin-binding growth factors. *J Control Rel* 65, 389-402, 2000.
21. Miller MJ, Khoo A, Thomson RC, Lemon JC, Gurlek A, Mikos AG. In vivo fabrication of vascularized tissue scaffolds. Presented at 43rd Annual Meeting of the Plastic Surgery Research Council, Loma Linda, CA, 1998.



**Author Information**

**Timothy W. King, MD, PhD**

Laboratory of Reparative Biology & Bioengineering, Department of Plastic Surgery, University of Texas M.D. Anderson Cancer Center

**Carol Johnston, HT (ASCP)**

Laboratory of Reparative Biology & Bioengineering, Department of Plastic Surgery, University of Texas M.D. Anderson Cancer Center

**Priscilla B. Chauvin, BS**

Division of Surgery, University of Texas M.D. Anderson Cancer Center

**Christine L. Tock, MD, PhD**

University of Pittsburgh Medical Center

**Gregory R. Reece**

Laboratory of Reparative Biology & Bioengineering, Department of Plastic Surgery, University of Texas M.D. Anderson Cancer Center

**Charles W. Patrick, Jr., PhD**

Laboratory of Reparative Biology & Bioengineering, Department of Plastic Surgery, University of Texas M.D. Anderson Cancer Center